Approximate Partial-Penetration Pseudoskin for Infinite-Conductivity Wells

Paul Papatzacos, SPE, Rogaland Research Inst.

SPE 13956

Summary. This paper presents a simple formula for the pseudoskin factor of a well with restricted flow entry where infinite conductivity is taken into account analytically. Comparisons with previously published results are shown graphically and in tabulated form.

Introduction

The concept of pseudoskin appears naturally in calculations of the pressure drop in an infinite slab reservoir with a well that is either partially penetrating or has limited flow entry. It is, in the semilog flow regime, the additional pressure drop that arises at the wellbore when the interval open to flow is smaller than the reservoir thickness.

Ref. 1 provides a comprehensive list and analysis of the extensive literature on the subject before 1975. For papers published since 1975, see Ref. 2 and its references.

The analytical calculation of the pressure drop is relatively straightforward for uniform-flux wells. For infinite-conductivity wells, however, there arise mathematical difficulties first identified by Muskat.[3] The earliest results on partial-penetration pseudoskin were presented graphically by Brons and Marting.[4] The calculations were based on a uniform-flux well and Muskat's method to approximate the infinite-conductivity situation (see Ref. 1).

Streltsova-Adams[5] presented explicit equations for pseudoskin caused by restricted flow entry in the form of infinite series. Streltsova-Adams uses a uniform-flux well and calculates an average pressure drop at the wellbore by integrating along the interval open to flow. Finally, Odeh[6] presented a simple equation. Refs. 5 and 6 assume anisotropic reservoirs. In Ref. 5, pseudoskin is expressed in terms of three dimensionless parameters (see Fig. 1):

$$h_{pD}=h_p/h_t, \quad \ldots\ldots\ldots\ldots\ldots\ldots\ldots\ldots\ldots\ldots (1)$$

$$r_D=\frac{r_w}{h_t}\left(\frac{k_V}{k_H}\right)^{1/2}, \quad \ldots\ldots\ldots\ldots\ldots\ldots\ldots\ldots\ldots\ldots (2)$$

and

$$h_{1D}=h_1/h_t. \quad \ldots\ldots\ldots\ldots\ldots\ldots\ldots\ldots\ldots\ldots (3)$$

An isotropic reservoir was assumed in Ref. 4, but Refs. 7 and 8 show that the Brons-Marting charts can be used for anisotropic reservoirs, provided one uses r_D instead of r_w/h_t.

Numerical values of pseudoskin for chosen values of h_{pD}, r_D, and h_{1D} where infinite conductivity has been accounted for numerically can be found in Refs. 2 and 7. Both references will be considered later in this paper as a basis for comparison.

Result of the Theoretical Analysis

The theoretical analysis presented in this paper is based on a result, derived in Ref. 9, concerning an infinite-conductivity well in an infinite reservoir. This result is used, together with the method of images,[10] to obtain the steady-state pressure drop at the wellbore of a well with restricted flow entry in a slab reservoir. The following equation is thus found, expressing pseudoskin in terms of h_{pD}, r_D, and h_{1D} defined previously:

$$s_p=\left(\frac{1}{h_{pD}}-1\right)\ln\frac{\pi}{2r_D}+\frac{1}{h_{pD}}\ln\left[\frac{h_{pD}}{2+h_{pD}}\left(\frac{A-1}{B-1}\right)^{1/2}\right], \quad \ldots\ldots\ldots\ldots (4)$$

where

$$A=1/(h_{1D}+h_{pD}/4) \quad \ldots\ldots\ldots\ldots\ldots\ldots\ldots\ldots\ldots\ldots (5)$$

and

$$B=1/(h_{1D}+3h_{pD}/4). \quad \ldots\ldots\ldots\ldots\ldots\ldots\ldots\ldots\ldots\ldots (6)$$

The derivation of Eq. 4 is given in Appendix A. As mentioned previously, it relies on the method of images, which uses, in addition to the physical well, an infinite number of image wells to generate the no-flow condition at the top and bottom of the reservoir. The steady-state pressure drop caused by any well is known.[9] The real well contributes a pressure drop that is constant along its own wellbore. Each image well, however, contributes a pressure drop that necessarily varies along the wellbore of the real well so that the method of images will not yield the exact infinite-conductivity solution. It will be shown, however, that Eq. 4 gives a good approximation in most cases of practical interest.

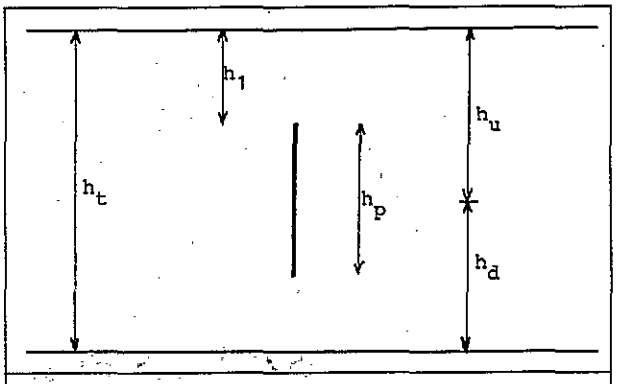

Fig. 1—Geometry and notation, infinite slab reservoir.

Comparison With Existing Results

A comparison is presented in Figs. 2 and 3 of Eq. 4 with the pseudoskin equations of Streltova-Adams[5] and of Odeh,[6] and also with the Brons-Marting charts.[4] The value of r_D is 0.01 and two main cases are explored: partial penetration (Fig. 2) and limited flow entry with a centrally located producing interval (Fig. 3). Deviations are usually small, especially between the numbers given by Eq. 4 and those given by the Streltova-Adams equation or the Brons-Marting charts.

Table 1 shows a comparison of Eq. 4 with numerical values published by Reynolds *et al.*[2] and by Bilhartz and Ramey.[7] Agreement is seen to be quite good. The origin of the large discrepancies that occur in some instances is discussed below.

Validity of the Solution

The derivation of Eq. 4 is based on the assumption of a line-source well. The introduction of a nonzero well radius causes an error that is small only if the well radius is small compared to the interval open to flow (see Appendix A).

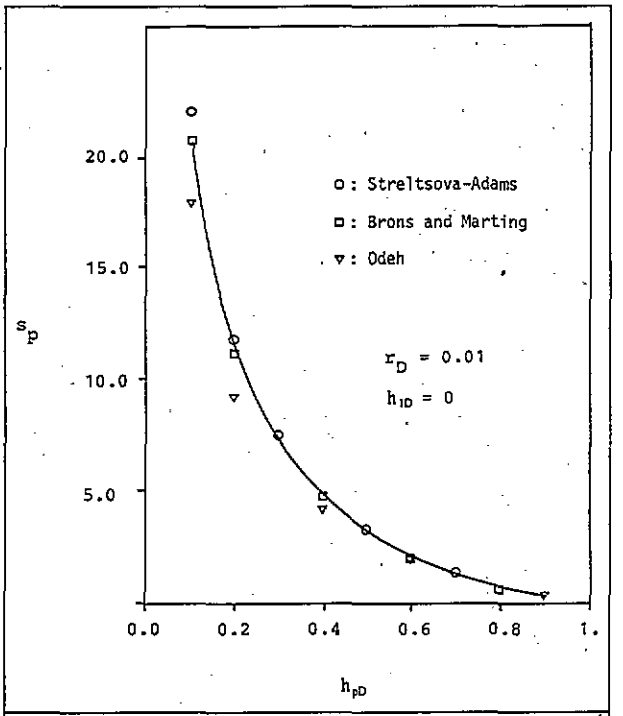

Fig. 2—Pseudoskin vs. h_{pD} when $h_{1D}=0$. Full line is Eq. 4.

In other words, the ratio r_D/h_{pD} should be small. According to the figures in Table 1 for $r_D=0.1000$, this ratio should be less than about 0.2.

As already mentioned, the method of images has introduced another source of error because each image well contributes a pressure drop that varies along the wellbore of the real well. This variation increases as h_p increases toward h_t. This effect is offset, however, by the requirement that s_p have the correct value, namely zero, when $h_p=h_t$, so that no dramatic loss of accuracy is expected as h_{pD} approaches 1.

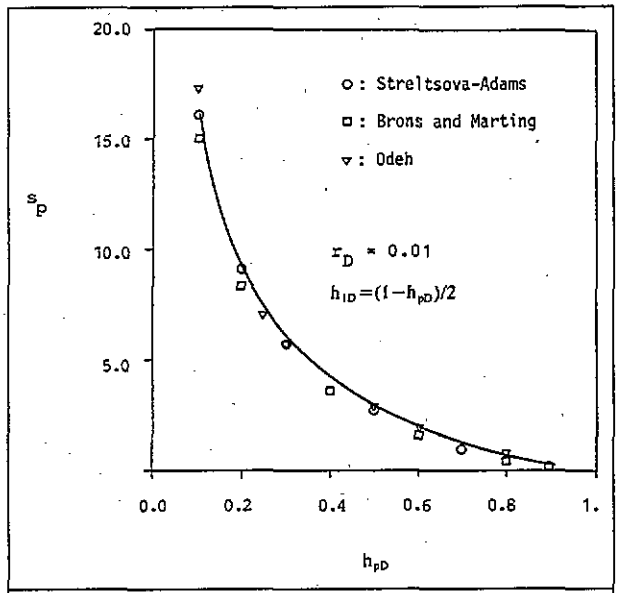

Fig. 3—Pseudoskin vs. h_{pD}, centrally perforated well. Full line is Eq. 4.

TABLE 1—COMPARISON OF PSEUDOSKIN CALCULATIONS

h_{pD}	r_D	Ref. 8 Calculated Value	Ref. 2 Calculated Value	Eq. 4 Calculated Value
0.10	0.0010	41.43	41.62	41.55
	0.0100	—	21.63	20.82
	0.1000	—	6.82	0.10
0.20	0.0010	—	20.46	20.48
	0.0100	—	11.35	11.27
	0.1000	—	3.92	2.06
0.25	0.00025	19.94	—	19.93
	0.0005	17.83	—	17.85
	0.0010	15.71	—	15.77
	0.0025	12.88	—	13.02
0.40	0.0010	—	8.15	8.25
	0.0100	—	4.68	4.79
	0.1000	—	1.73	1.34
0.50	0.0005	6.17	—	6.27
	0.0010	5.47	—	5.58
	0.0020	4.75	—	4.88
	0.0050	3.79	—	3.97
0.60	0.0010	—	3.61	3.74
	0.0100	—	2.05	2.21
	0.1000	—	0.73	0.67

Conclusions

Eq. 4 gives a simple and reliable means to calculate pseudoskin for wells with limited flow entry as long as the ratio $r_D/h_{pD} < \sim 0.2$. This condition is satisfied in the majority of cases because usually $k_V < k_H$ while $r_w/h_p < \sim 0.1$.

A detailed investigation of the accuracy afforded by Eq. 4 in all situations, especially for nonzero h_{1D}, has not been possible because, to the best of my knowledge, no numerical values for pseudoskin have been published other than those included in Table 1.

Nomenclature

$a_n(z_D)$ = defined in Eq. A-8, dimensionless
$A; B$ = dimensionless constants defined in Eqs. 5 and 6
A_1, A_2, A_3, A_4 = dimensionless constants defined in Eq. A-15
B_1, B_2, B_3, B_4 = dimensionless constants defined in Eq. A-16
c_t = total reservoir compressibility, psi^{-1} [kPa^{-1}]
F = argument of logarithm in Eq. A-21, defined in Eq. A-22, dimensionless
h_d = height from middle of producing interval to bottom of reservoir, ft [m]
h_p = height of producing interval, ft [m]
h_{pD} = dimensionless h_p (see Eq. 1)
h_t = reservoir thickness, ft [m]
h_u = height from top of reservoir to middle of producing interval, ft [m]
h_1 = height from top of reservoir to top of producing interval, ft [m]
h_{1D} = dimensionless h_1 (see Eq. 3)
$\Delta h_t, \Delta h_u, \Delta h_d$ = defined in Eq. A-11, dimensionless
k_H, k_V = horizontal and vertical permeabilities, respectively, md
L = dimensionless constant defined in Eq. A-23
N = half-number of image wells
p = reservoir pressure, psi [kPa]
p_D^{∞} = dimensionless pressure in infinite reservoir (see Eq. A-1)
p_i = initial reservoir pressure, psi [kPa]
p_w = wellbore pressure, psi [kPa]
p_{wD} = wellbore pressure, dimensionless (see Eq. A-3)
p_{wD}^{∞} = dimensionless wellbore pressure in infinite reservoir (see Eq. A-3)
p_{wDV} = dimensionless wellbore pressure in slab reservoir caused by image wells (see Eq. A-3)
p_{wDV1}, p_{wDV2} = dimensionless Stages 1 and 2 values of p_{wDV} (see Eq. A-12)
q = well volumetric flow rate, RB/D [res m^3/d]
r_D = dimensionless radius defined in Eq. 2
Δr_D = dimensionless radial distance (see Eq. B-3)
r_w = wellbore radius, ft [m]
s = Laplace parameter, dimensionless
s_p = pseudoskin, dimensionless
t = time, hours
t_D = dimensionless time (see Eq. B-1)
U = unknown dimensionless constant equal to

$$\sum_0^{\infty} \beta_m \tau^{2m+1}$$

(see Eqs. A-27 and A-28)
U' = unknown dimensionless constant equal to $\ln \tau + 2U$ (see Eq. A-29)
U_n = dimensionless constant defined in Eq. A-14
V_n = dimensionless constant defined in Eq. A-18
x,y,z = Cartesian coordinates, ft [m]
x_D, y_D, z_D = dimensionless Cartesian coordinates (see Eq. B-1)
α,β = angular prolate spheroidal coordinates (see Eq. B-2), dimensionless
α_n = dimensionless constant in Eq. A-9
β_m = dimensionless constant in Eq. A-27
γ = Euler constant=0.5772
Γ = gamma function
μ = oil viscosity, cp [Pa·s]
ξ = prolate spheroidal coordinate (see Eq. B-2), dimensionless
ξ_w = value of ξ at the wellbore, dimensionless
τ = dimensionless constant (see Eq. A-2)
ϕ = reservoir porosity, fraction

Subscripts

i,m,n = integers used as both indices and powers

Acknowledgments

I am grateful to Leif Larsen of Rogalandsforskning for numerous discussions and comments during the writing of this paper, and to Trond Unneland of Statoil for permission to use his work in Figs. 2 and 3.

References

1. Gringarten, A.C. and Ramey, H.J. Jr.: "An Approximate Infinite Conductivity Solution for a Partially Penetrating Line-Source Well," *SPEJ* (April 1975) 140–48.
2. Reynolds, A.C., Chen, J., and Raghavan, R.: "Pseudoskin Factor Caused by Partial Penetration," *JPT* (Dec. 1984) 2197–2210.
3. Muskat, M.: *Physical Principles of Oil Production*, Intl. Human Resources Development Corp., Boston (1981).
4. Brons, F. and Marting, V.E.: "The Effect of Restricted Flow Entry on Well Productivity," *JPT* (Feb. 1961) 172–74.
5. Streltsova-Adams, T.D.: "Pressure Drawdown in a Well With Limited Flow Entry," *JPT* (Nov. 1979) 1469–76.

6. Odeh, A.S.: "An Equation for Calculating Skin Factor Due to Restricted Entry," *JPT* (June 1980) 964–65.
7. Bilhartz, H.L. Jr. and Ramey, H.J. Jr.: "The Combined Effects of Storage, Skin and Partial Penetration on Well Test Analysis," paper SPE 6753 presented at the 1977 SPE Annual Technical Conference and Exhibition, Denver, Oct. 9–12.
8. Kazemi, H. and Seth, S.M.: "Effect of Anisotropy and Stratification on Pressure Transient Analysis of Wells with Restricted Flow Entry," *JPT* (May 1969) 639–47.
9. Papatzacos, P.: "Exact Solutions for Infinite-Conductivity Wells," paper SPE 13846 available from SPE, Richardson, TX.
10. Nisle, R.G.: "The Effect of Partial Penetration on Pressure Buildup in Oil Wells," *Trans.*, AIME (1958) **213**, 85.
11. Flammer, C.: *Spheroidal Wave Functions*, Stanford U. Press, Stanford, CA (1957).
12. Gradshteyn, I.S. and Ryzhik, I.M.: "Tables of Integrals Series and Products," Academic Press, New York City (1965).
13. Whittaker, E.T. and Watson, G.N.: *A Course of Modern Analysis*, Cambridge U. Press, London (1965) Sec. 12.13.
14. Abramowitz, M. and Stegun, I.A.: *Handbook of Mathematical Functions*, Dover Publications Inc., New York City (1972).
15. Matthews, C.S. and Russel, D.G.: *Pressure Buildup and Flow Tests in Wells*, Monograph Series, SPE, Richardson (1967) 1.

Appendix A: Derivation of the Pseudoskin Formula

This paper is an application of an earlier result[9] stating that the pressure drop around an infinite-conductivity line-source well in an infinite reservoir is given for large times by

$$p_i - p = 141.2 \frac{2\mu q}{h_p k_H} p_D^\infty, \qquad \text{(A-1a)}$$

where

$$p_D^\infty = \tfrac{1}{2} \ln \frac{e^\xi + 1}{e^\xi - 1} \qquad \text{(A-1b)}$$

and ξ is a prolate spheroidal coordinate (see Appendix B, where dimensionless coordinates and dimensionless time are also defined).

The main idea is to use Eq. A-1 with the method of images[10] to obtain the pressure drop in the vicinity of the well and hence the pseudoskin in the realistic situation of a slab reservoir (i.e., areally infinite, with no-flow conditions at the upper and lower boundaries). The method of images is illustrated in Fig. A-1. The interval open to flow of the real well is placed arbitrarily relative to the top of the slab-like reservoir. The image wells are then all production wells placed in such a way as to produce no-flow surfaces coinciding with the top and bottom of the reservoir.

There are an infinite number of image wells, and this is the cause of the main technical difficulty encountered in the calculation: the sum of their contributions will diverge. One does expect a divergence because it is known from calculations with uniform-flux wells[5] that the pressure drop behaves as ln t_D for large t_D. It will thus be necessary in the course of the calculation to isolate the divergence and to identify the pseudoskin factor in the remaining terms. This will be done by the following method.

Instead of an infinite number of wells, the calculation will be started with a finite, but very large, number, $2N$, of image wells, N above and N below the real well. In addition, the time, t_D, will be taken to be very large but finite. The pressure drop caused by the image wells will then be obtained by summing a finite number of terms and will itself be finite. It will contain an easily identifiable term, however, which will diverge when $N \to \infty$. After the divergence is isolated, N and t_D will be made infinite, thus giving the pressure drop in a form wherein pseudoskin can be read. As it turns out, it is important to know how N and t_D grow to infinity relative to each other.

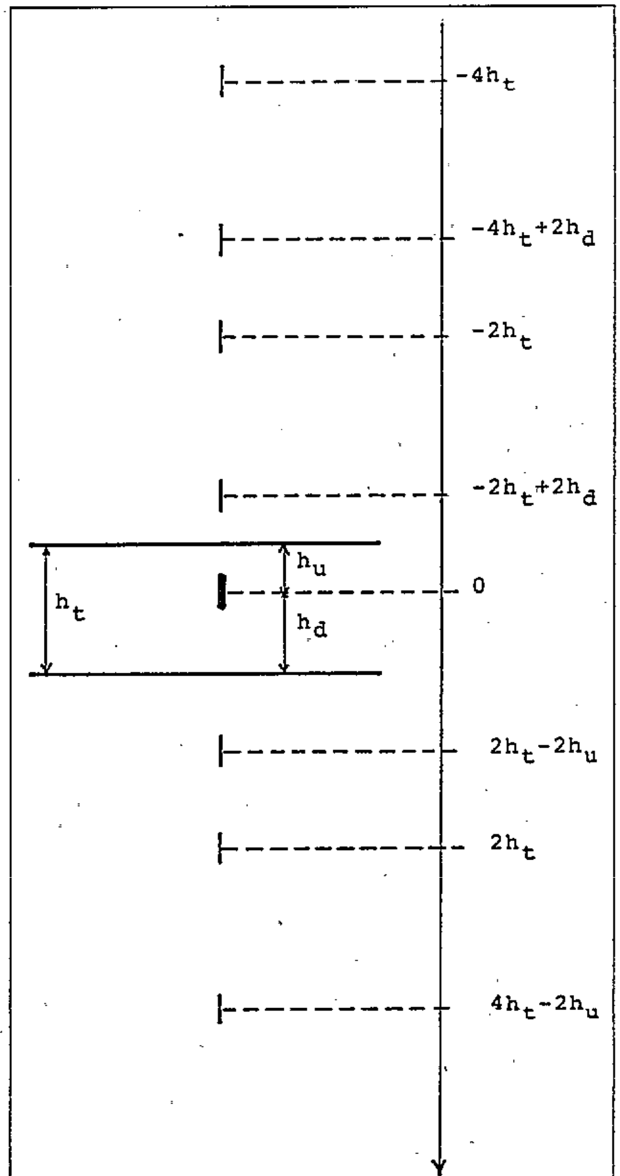

Fig. A-1—Illustration of the method of images. Distances from the real well to the image wells are given on the vertical axis (positive downward).

Consider the Nth image well (above or below the real well). It is roughly a distance Nh_t from the real well (see Fig. A-1). If the pressure drop caused by this image well at the real well is to be obtained from Eq. A-1, then the time, t, must be much larger than the time it takes a transient to cover the distance Nh_t. In dimensionless form the latter is on the order of $(2Nh_t/h_p)^2$, so that the condition $t_D >> (2Nh_t/h_p)^2$ must be fulfilled. Thus the calculations must be done at a time $t_D >> 1$ and with a value of $N >> 1$ such that

$$\frac{2Nh_t}{h_p \sqrt{t_D}} = \tau << 1. \qquad \text{(A-2)}$$

Eventually, t_D and N must go to infinity in such a way that τ remains constant.

The pressure drop at the wellbore of an infinite-conductivity line-source well in a slab reservoir can be expressed as

$$p_i - p_w = 141.2 \frac{\mu q}{h_t k_H} p_{wD}, \quad \ldots\ldots\ldots\ldots\ldots \text{(A-3a)}$$

where

$$p_{wD} = p_{wD}^{\infty} + p_{wDV}, \quad \ldots\ldots\ldots\ldots\ldots\ldots \text{(A-3b)}$$

where the two terms on the right side of Eq. A-3b are the contributions at the wellbore of the real well, from the real well and the totality of the image wells, respectively. The rest of this Appendix is devoted to the calculation of these two terms.

Preliminary Result 1: A Model of the Real Well. One of the assumptions underlying Eqs. A-1 is that of a line-source well. It follows that the pressure drop at the wellbore of the real well caused by the real well itself is infinite. To avoid this spurious infinity, it is necessary to assume that the real well is a thin ellipsoid, given by $\xi = \xi_w << 1$. Eqs. A-1 then give the first term on the right side of Eqs. A-3:

$$p_{wD}^{\infty} = \tfrac{1}{2} \ln(2/\xi_w). \quad \ldots\ldots\ldots\ldots\ldots\ldots \text{(A-4)}$$

It is now necessary to express ξ_w in terms of the familiar parameters of a well—i.e., the length of the interval open to flow and the radius. The value ξ_w is determined by requiring that the ellipsoid have a long axis equal to h_p and the surface equal to the lateral surface of a cylinder with radius r_w and height h_p. One finds that

$$\xi_w \approx \frac{8}{\pi} \left(\frac{k_V}{k_H} \right)^{1/2} \frac{r_w}{h_p} = \frac{8}{\pi} \frac{r_D}{h_{pD}}. \quad \ldots\ldots\ldots\ldots \text{(A-5)}$$

By combining Eqs. A-4 and A-5, one gets the first term on the right side of Eq. A-3b:

$$p_{wD}^{\infty} = -\tfrac{1}{2} \ln \left(\frac{4}{\pi} \frac{r_D}{h_{pD}} \right). \quad \ldots\ldots\ldots\ldots\ldots \text{(A-6)}$$

Because ξ_w is assumed to be small, the calculations to follow are valid only for wells where the right side of Eq. A-5 is small.

Preliminary Result 2: Pressure Drop From an Image Well on its Axis Away From its Own Wellbore. Because real and image wells are along the z_D axis, the contribution to the pressure drop from an image well at the real well is found from Eqs. A-1 by specializing to $\Delta r_D = 0$ (implied by $\xi_w << 1$) and by choosing the appropriate z_D. It follows from Eqs. B-2 and B-3 that $\cosh \xi = z_D$, which, when used in Eqs. A-1, results in

$$p_D^{\infty}(\Delta r_D = 0, z_D) = \tfrac{1}{4} \ln \frac{z_D + 1}{z_D - 1}. \quad \ldots\ldots\ldots\ldots \text{(A-7)}$$

To simplify, $\Delta r_D = 0$ will be dropped hereafter.

As mentioned at the beginning of this Appendix, the calculations must first be performed with $t_D >> 1$ but finite. Eq. A-7 is valid in the limit $t_D \to \infty$ and is thus not sufficient; what is actually required is an asymptotic expansion of $p_D^{\infty}(z_D, t_D)$. The pressure drop around an infinite-conductivity well in an infinite reservoir is known in terms of its Laplace transform,[9] given in the form of an infinite series where each term is a rational function of spheroidal wave functions. An asymptotic expansion valid for large t_D can be obtained by expanding the Laplace transform in powers of the Laplace parameter, s, around $s = 0$, then inverting term by term. One then finds (see Ref. 11 for the necessary equations on spheroidal wave functions)

$$p_D^{\infty}(z_D, t_D) = \tfrac{1}{4} \ln \frac{z_D + 1}{z_D - 1} + \sum_{n=0}^{\infty} \frac{a_n(z_D)}{t_D^{n+1/2}}, \quad \ldots \text{(A-8)}$$

where $a_n(z_D)$ can be obtained, but the calculations are extremely laborious when $n > 1$. It will later be shown that it is not necessary to know a_n explicitly. It is sufficient to know their behavior for large z_D. The following properties will be assumed: (1) for large z_D, $a_n(z_D)$ has the form

$$a_n(z_D) = \alpha_n z_D^{2n}, \quad \ldots\ldots\ldots\ldots\ldots\ldots \text{(A-9)}$$

and (2) the coefficient α_n in Eq. A-9 is a constant (independent of ξ_w).

It is relatively easy to check that the above assumptions are verified by a_0 and a_1. Physical reasons also support these assumptions, as will be shown later.

The second term on the right side of Eq. A-3b is a sum of terms, such as Eq. A-8, each with the appropriate z_D. Referring to Fig. A-1, one sees that

$$p_{wDV} = \sum_{n=1}^{N/2} [p_D^{\infty}(4n\Delta h_t - 4\Delta h_d + z_D, t_D) + p_D^{\infty}(4n\Delta h_t + z_D, t_D) + p_D^{\infty}(4n\Delta h_t - 4\Delta h_u - z_D, t_D) + p_D^{\infty}(4n\Delta h_t - z_D, t_D)], \quad \ldots\ldots\ldots\ldots \text{(A-10)}$$

where

$$\Delta h_t = h_t / h_p, \quad \ldots\ldots\ldots\ldots\ldots\ldots \text{(A-11a)}$$

$$\Delta h_u = h_u / h_p, \quad \ldots\ldots\ldots\ldots\ldots\ldots \text{(A-11b)}$$

and

$$\Delta h_d = h_d / h_p = \Delta h_t - \Delta h_u, \quad \ldots\ldots\ldots\ldots \text{(A-11c)}$$

and where p_D^{∞} is given by Eq. A-8. Eq. A-8 also shows that the actual calculation of p_{wDV} has two stages: a first

stage where one sums the logarithmic part of p_D^{∞} and a second stage where one considers the time-dependent part of p_D^{∞}. Thus,

$$p_{wDV}=p_{wDV1}+p_{wDV2}. \quad \text{(A-12)}$$

Pressure Drop Caused by Image Wells: First Stage of the Calculation. From Eq. A-10, with the notation introduced in Eq. A-12, one obtains

$$p_{wDV1}=\tfrac{1}{4}\sum_{n=1}^{N/2} U_n, \quad \text{(A-13)}$$

where U_n is given by the following:

$$U_n=\ln\left[\frac{(1+A_1/n)(1+A_2/n)(1+A_3/n)(1+A_4/n)}{(1-B_1/n)(1-B_2/n)(1-B_3/n)(1-B_4/n)}\right], \quad \text{(A-14)}$$

where

$$A_1=\frac{1+z_D-4\Delta h_d}{4\Delta h_t}, \quad \text{(A-15a)}$$

$$A_2=\frac{1+z_D}{4\Delta h_t}, \quad \text{(A-15b)}$$

$$A_3=\frac{1-z_D-4\Delta h_u}{4\Delta h_t}, \quad \text{(A-15c)}$$

and

$$A_4=\frac{1-z_D}{4\Delta h_t}; \quad \text{(A-15d)}$$

and

$$B_1=\frac{1-z_D+4\Delta h_d}{4\Delta h_t}, \quad \text{(A-16a)}$$

$$B_2=\frac{1-z_D}{4\Delta h_t}, \quad \text{(A-16b)}$$

$$B_3=\frac{1+z_D+4\Delta h_u}{4\Delta h_t}, \quad \text{(A-16c)}$$

and

$$B_4=\frac{1+z_D}{4\Delta h_t}. \quad \text{(A-16d)}$$

The sum (Eq. A-13) is divergent when $N\to\infty$, and the divergence can be isolated as will now be shown. Noting that

$$U_n=\frac{2}{n\Delta h_t}+\ldots(n\to\infty), \quad \text{(A-17)}$$

one defines V_n by

$$U_n=\frac{2}{n\Delta h_t}+V_n, \quad \text{(A-18)}$$

whereby Eq. A-13 becomes

$$p_{wDV1}=\frac{1}{2\Delta h_t}\sum_{n=1}^{N/2}\frac{1}{n}+\tfrac{1}{4}\sum_{n=1}^{N/2} V_n. \quad \text{(A-19)}$$

The first sum on the right side is known.[12] Moreover, because V_n behaves as $1/n^2$ for large n, one obtains

$$p_{wDV1}=\frac{1}{2\Delta h_t}\left(\ln\frac{N}{2}+\gamma\right)+\tfrac{1}{4}\sum_{n=1}^{\infty} V_n+0(1/N), \quad \text{(A-20)}$$

where γ is Euler's constant (0.5772). It now remains to evaluate the sum over V_n. This is done by using a method given in Ref. 13. The result is

$$\tfrac{1}{4}\sum_{n=1}^{\infty} V_n=-\frac{\gamma}{2\Delta h_t}+\tfrac{1}{4}\ln\left[\frac{\prod_{i=1}^{4}\Gamma(1-B_i)}{\prod_{i=1}^{4}\Gamma(1+A_i)}\right], \quad \text{(A-21)}$$

where Γ is the gamma function. The argument of the logarithm in Eq. A-21 will be denoted by F. A much simpler expression for F can be found when one makes use of the properties of the gamma function,[14] especially the fact that $\ln[\Gamma(x)]$ varies very little when $1<x<2$. This simpler form given below is only an approximation. It achieves, however, a relative accuracy for the pseudoskin on the order of 1% in all cases of interest.

$$F=2^{2/\Delta h_t}[L(\Delta h_t,\Delta h_u,z_D)]^2, \quad \text{(A-22)}$$

where

$$L(\Delta h_t,\Delta h_u,z_D)=2\Delta h_t\times\left\{\frac{(2\Delta h_t+1)^2-(z_D-2\Delta h_d+2\Delta h_u)^2}{[(2\Delta h_t+1)^2-z_D^2][(2\Delta h_t-1)^2-(z_D-2\Delta h_d+2\Delta h_u)^2]}\right\}^{1/2} \quad \text{(A-23)}$$

It follows that Eq. A-20 can be written as

$$p_{wDV1}=\frac{1}{2\Delta h_t}\ln N+\tfrac{1}{2}\ln L(\Delta h_t,\Delta h_u,z_D)+0(1/N). \quad \ldots\ldots\ldots\ldots\ldots\ldots\ldots\ldots\ldots\ldots \text{(A-24)}$$

It is now evident that p_{wDV1} is a function of z_D, so Eq. 4 will not be a rigorous infinite-conductivity solution. (It will be shown soon that there is no other z_D dependence.) This z_D dependence will eventually be eliminated.

Pressure Drop Caused by Image Wells: Second Stage of the Calculation. p_{wDV2} will now be calculated. Referring to Eqs. A-12, A-10, and A-8, one finds

$$p_{wDV2}=\sum_{n=1}^{N/2}\left\{\sum_{m=0}^{\infty}\left[\frac{a_m(4n\Delta h_t-4\Delta h_d+z_D)}{t_D{}^{m+\frac{1}{2}}}+\frac{a_m(4n\Delta h_t+z_D)}{t_D{}^{m+\frac{1}{2}}}+\frac{a_m(4n\Delta h_t-4\Delta h_u-z_D)}{t_D{}^{m+\frac{1}{2}}}+\frac{a_m(4n\Delta h_t-z_D)}{t_D{}^{m+\frac{1}{2}}}\right]\right\}. \quad \ldots\ldots\ldots\ldots\ldots\ldots \text{(A-25)}$$

It is now assumed that no error is introduced by changing the order of summation, and the n summation is performed first. By using Eq. A-9 and concentrating on the leading order in N, one finds

$$\sum_{n=1}^{N/2} a_m(4n\Delta h_t+\ldots)$$

$$=\sum_{n=1}^{N/2}[\alpha_m n^{2m}(4\Delta h_t)^{2m}+\ldots]$$

$$=\alpha_m(4\Delta h_t)^{2m}\frac{(N/2)^{2m+1}}{2m+1}[1+0(1/N)]. \quad \ldots\ldots \text{(A-26)}$$

By combining Eqs. A-25 and A-26, one finds

$$p_{wDV2}=\frac{1}{\Delta h_t}\sum_{m=0}^{\infty}\beta_m\left(\frac{2N\Delta h_t}{\sqrt{t_D}}\right)^{2m+1}[1+0(1/N)], \quad \ldots\ldots\ldots\ldots\ldots\ldots\ldots\ldots \text{(A-27)}$$

where β_m is a real number, independent of ξ_w (see Assumption 2 after Eq. A-9).

Pressure Drop at Large Times: Final Result. One can now combine Eqs. A-3, A-24, and A-27 to obtain the pressure drop caused by the image wells. According to the rule mentioned at the beginning, N and t_D will be made to go to infinity in such a way that τ, given by Eq. A-2, remains constant. One then sees from Eq. A-24 that

$$p_{wDV1}=\frac{1}{4\Delta h_t}\ln t_D-\frac{1}{2\Delta h_t}\ln(2\Delta h_t)+\tfrac{1}{2}\ln L(\Delta h_t,\Delta h_u,z_D)+\frac{1}{2\Delta h_t}\ln\tau$$

and from Eq. A-27 that

$$p_{wDV2}=\frac{U}{\Delta h_t}, \quad \ldots\ldots\ldots\ldots\ldots\ldots\ldots\ldots \text{(A-28)}$$

where U is an unknown number, depending on τ. It then follows that

$$p_{wDV}=\frac{1}{4\Delta h_t}\ln t_D-\frac{1}{2\Delta h_t}\ln(2\Delta h_t)+\tfrac{1}{2}\ln L(\Delta h_t,\Delta h_u,z_D)+\frac{U'}{2\Delta h_t}, \quad \ldots\ldots\ldots \text{(A-29)}$$

where $U'=\ln\tau+2U$ is a number, depending on the choice of τ. That U' is a constant follows from Eq. A-8 and from the assumptions made thereafter about a_n. If the assumption of Eq. A-9 is not verified, perhaps if the a_n diverge more severely than assumed for large z_D, then the pressure drop will have a more severe divergence than the logarithmic one shown in Eq. A-28. Further, Assumption 2 following Eq. A-9 implies than U' does not, in particular, depend on ξ_w, which is physically correct because Eq. A-28 gives the image-well contribution; the pressure drop far from the wellbore does not significantly depend on the well radius.

It remains that U' is a constant that must be determined, which is done below. By combining Eqs. A-3, A-6, and A-29 and by taking Eqs. A-1 into account, one obtains

$$p_{wD}=-\Delta h_t\ln\left(\frac{4}{\pi}\frac{r_D}{h_{pD}}\right)+\tfrac{1}{2}\ln\frac{4k_V t}{\phi\mu c_t h_p^2}-\ln(2\Delta h_t)+\Delta h_t\ln L(\Delta h_t,\Delta h_u,z_D)+U'. \quad \ldots\ldots\ldots\ldots \text{(A-30)}$$

The usual expression defining skin is[15]

$$p_{wD}=\tfrac{1}{2}\ln\frac{4k_H t}{\phi\mu c_t r_w^2}-\frac{\gamma}{2}+s_p. \quad \ldots\ldots\ldots\ldots \text{(A-31)}$$

One then obtains a formula for the pseudoskin by identifying Eq. A-30 with Eq. A-31. The expression thus obtained contains the arbitrary constant U' and depends on z_D. These two constants are determined by the condition that $s_p=0$ when $\Delta h_t=1$. In this case, the best choice is $z_D=0$, and one then finds

$$U'=\ln(4/\pi)-\gamma/2.$$

The final expression for the pseudoskin is

$$s_p=(\Delta h_t-1)\ln\frac{\pi}{2r_D}$$

$$+\Delta h_t\ln\left\{\frac{1}{2\Delta h_t+1}\left[\frac{(4\Delta h_u+1)(4\Delta h_d+1)}{(4\Delta h_u-1)(4\Delta h_d-1)}\right]^{1/2}\right\}, \quad \ldots\ldots\ldots\ldots\ldots\ldots\ldots\ldots\ldots\ldots \text{(A-32)}$$

where Δh_t, Δh_d, and Δh_u are given by Eq. A-11 (see also Fig. 1).

Eq. 4 is recovered when the more familiar parameters, h_{pD} and h_{1D}, are used in Eq. A-32.

Appendix B—Prolate Spheroidal Coordinates

Dimensionless coordinates x_D, y_D, and z_D and dimensionless time, t_D, are defined as follows, in accordance with Ref. 10:

$$x_D=(k_V/k_H)^{1/2}(2x/h_p), \quad \ldots\ldots\ldots\ldots\ldots\ldots\ldots\ldots \text{(B-1a)}$$

$$y_D=(k_V/k_H)^{1/2}(2y/h_p), \quad \ldots\ldots\ldots\ldots\ldots\ldots\ldots\ldots \text{(B-1b)}$$

$$z_D=2z/h_p, \quad \ldots\ldots\ldots\ldots\ldots\ldots\ldots\ldots\ldots\ldots\ldots \text{(B-1c)}$$

and

$$t_D=2.367\times10^{-4}4k_Vt/(\phi\mu c_t h_p^2). \quad \ldots\ldots\ldots\ldots \text{(B-1d)}$$

The meanings of x, y, z, and h_p are given by Fig. B-1.

Prolate spheroidal coordinates[9] (ξ, α, and β) are related to the usual Cartesian by

$$x_D=\sinh\xi\sin\alpha\cos\beta, \quad \ldots\ldots\ldots\ldots\ldots\ldots\ldots \text{(B-2a)}$$

$$y_D=\sinh\xi\sin\alpha\sin\beta, \quad \ldots\ldots\ldots\ldots\ldots\ldots\ldots \text{(B-2b)}$$

and

$$z_D=\cosh\xi\cos\alpha. \quad \ldots\ldots\ldots\ldots\ldots\ldots\ldots\ldots\ldots \text{(B-2c)}$$

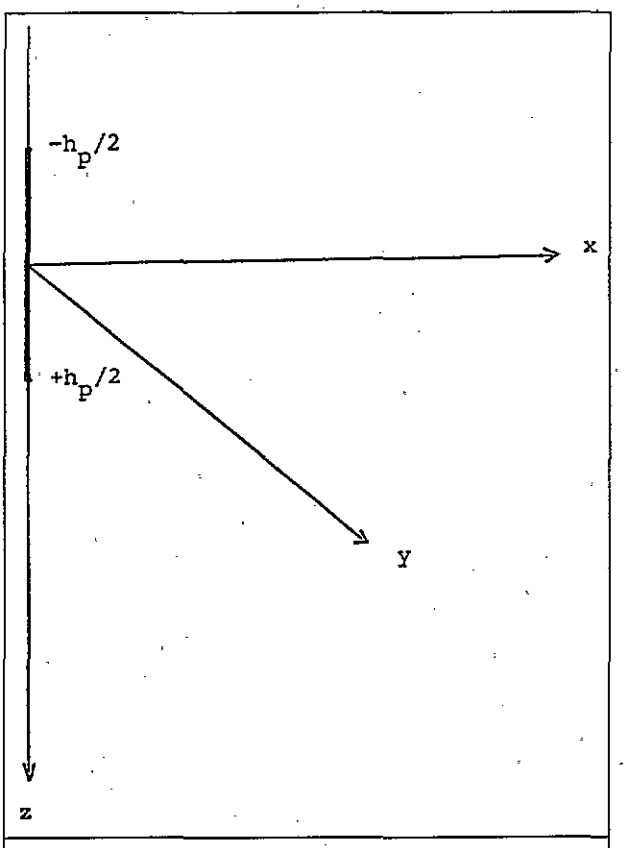

Fig. B-1—Cartesian coordinate system. The interval open to flow is represented by the thick line.

Because of rotational symmetry around the z_D axis, it is useful to introduce

$$\Delta r_D=(x_D^2+y_D^2)^{1/2}=\sinh\xi\sin\alpha. \quad \ldots\ldots\ldots\ldots \text{(B-3)}$$

The interval of the well open to flow is given by $\xi=0$.

SPERE

Original manuscript (SPE 13956) received in the Society of Petroleum Engineers office Jan. 16, 1985. Paper accepted for publication May 2, 1986. Revised manuscript received April 14, 1986.